Available online at www.sciencedirect.com
SCIENCE DIRECT®
Journal of Power Sources 140 (2005) 168–180
JOURNAL OF POWER SOURCES
www.elsevier.com/locate/jpowsour

Processes taking place in the paste of lead-acid battery plates during soaking prior to formation and their influence on battery performance

M. Dimitrov, D. Pavlov*, T. Rogachev, M. Matrakova, L. Bogdanova

Central Laboratory of Electrochemical Power Sources, Bulgarian Academy of Sciences, Acad. G. Bonchev Street, Block 10, Sofia 1113, Bulgaria

Received 19 March 2004; received in revised form 29 July 2004; accepted 16 August 2004
Available online 6 October 2004

Abstract

The soaking procedure is a step in the technological process of production of lead-acid battery plates. Cured plates are left to stay in the formation solution on open circuit (i.e. soaked) for 1–4 h and after that the formation process starts. During soaking, the cured paste undergoes partial sulfation. The changes in chemical and phase composition as well as the structure of the paste and the crystal morphology of plates prepared with 3BS pastes and soaked in 1.06 or 1.25 s.g. H_2SO_4 solution are investigated in the present work. It has been established that during soaking the lead oxides and basic lead sulfates in the paste are hydrated first and then sulfated forming 1BS and $PbSO_4$. The content of these phases decreases in the inner parts of the plates. This results in the formation of a heterogeneous structure and composition of the paste. The sulfation of the corrosion layer has also been investigated. Batteries with plates prepared with 3BS paste and PbSnCa grids have considerably longer cycle life, if soaked and formed in 1.06 s.g. H_2SO_4 solution as compared to those soaked and formed in 1.25 s.g. H_2SO_4 solution.

Keywords: Lead-acid battery; Lead-acid battery technology; Soaking of lead-acid battery plates in H_2SO_4 solution; Sulfation of lead oxides; Sulfation of 3BS paste; Structure of sulfated lead-acid battery paste

1. Introduction

During the production of lead-acid batteries, when pasted and cured plates are soaked in H_2SO_4 solution before formation, sulfuric acid reacts with the cured paste whereby the paste is sulfated. The reaction between H_2SO_4 and the paste proceeds in a reaction layer between the zones of cured paste and sulfated paste. With the time of soaking, the reaction layer advances into the bulk of the cured paste, thus the zone of sulfated paste grows in size, whereas the volume of cured paste decreases. Zone processes take place also during formation of the plates of lead-acid batteries [1–3].

It has been established that the processes of sulfation of the plates during soaking are influenced greatly by the concentration of H_2SO_4 and the phase composition of the cured paste [4–6]. Attempts have been made to find the optimum conditions of soaking [7,8]. The processes during soaking of 4BS plates have also been investigated as well as the sulfation of the bulk of 4BS crystals [9–12].

The aims of the present investigation are: (a) to disclose the mechanism of the processes that take place in the 3BS cured paste during plate soaking, (b) to find out how does the soaking process influence the macrostructure of the paste and of the paste/grid interface and (c) to establish what is the effect of the soaking process on battery cycle life.

2. Experimental

2.1. Plate preparation

The paste for the experimental plates was prepared through mixing commercial leady oxide (LO), water and H_2SO_4 (s.g. 1.40) in a ratio equal to 5% H_2SO_4/LO at 30 °C. The paste had a density of 4.15 g/cm^3 and was composed of 3BS, α and β-PbO, and Pb. Commercial grids cast from Pb–1.2%Sn–0.056%Ca–0.002%Al alloy were pasted, set to

* Corresponding author. Tel.: +359 271 8651; fax: +359 273 1552.
E-mail address: dpavlov@mbox.cit.bg (D. Pavlov).

0378-7753/$ – see front matter © 2004 Elsevier B.V. All rights reserved.
doi:10.1016/j.jpowsour.2004.08.006

curing at 50 °C and 98% RH for 18 h, and then dried at 60 °C and 60% RH for 5 h followed by another 4 h at 60 °C and 10% RH [13].

2.2. Investigation of the processes during plate soaking

Three cured positive plates were placed in a cell box with 1.06 s.g. H_2SO_4 or 1.25 s.g. H_2SO_4 solution. One plate was taken out from the box, washed and dried after 1, 2 and 4 h of soaking.

As the process of sulfation affects the different zones across the plate thickness to a different extent, each of the plates was divided in three sub-layers: (i) *outer sub-layer* on the plate surface contacting the solution, (ii) *central* (*inner*) *sub-layer* of the plate, and (iii) *intermediate sub-layer* between the above two. These three sub-layers were set to various analysis as follows:

(a) chemical analysis to determine the content of $PbSO_4$, PbO and Pb;
(b) X-ray diffraction analysis to determine the phase composition of the paste;
(c) SEM observations to examine the structure of the paste and the morphology of its crystals;
(d) differential scanning calorimetry (DSC) and thermogravimetric analysis (TGA) to measure the degree of hydration of the paste;
(e) BET surface measurements to determine the integral BET surface area of the plate;
(f) pore volume distribution by pore radius throughout the plate.

2.3. Battery cycle life tests

Cells were assembled with two positive plates, enveloped in 3 mm thick AGM separator, and three negative plates per cell. The thus assembled cells (under 20% compression) were filled with 1.06 or 1.25 s.g. H_2SO_4 solution. Six test batteries 12 V/21 A h (20 h discharge rate) were assembled and subjected to soaking for 1, 2 or 4 h, and then to formation in the same solution employing an algorithm developed in this laboratory. After formation, the solution was poured out and replaced with a fresh one of such a concentration as to obtain 1.28 s.g. final H_2SO_4 concentration in the cells. The batteries were set to three capacity tests and then to cycling at 3 h rate of discharge down to 100% DOD followed by 115% overcharge versus the preceding discharge cycle.

3. Experimental results and discussion

3.1. Changes in H_2SO_4 concentration during plate soaking

Fig. 1 shows the changes in H_2SO_4 concentration of solutions with 1.06 and 1.25 s.g. during soaking of the three positive plates. The volume of electrolyte per g paste was 1.6 ml of 1.06 s.g. H_2SO_4 and 1.0 ml of 1.25 s.g. H_2SO_4.

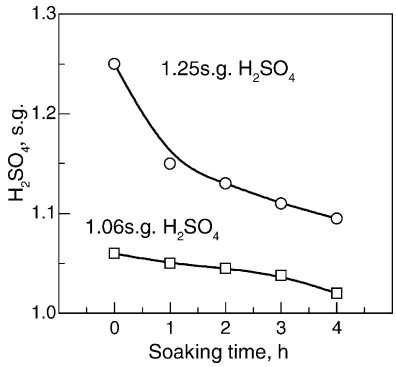

Fig. 1. Changes in H_2SO_4 concentration during plate soaking.

The higher the H_2SO_4 concentration the greater the changes in acid concentration during soaking. When the plates were soaked in H_2SO_4 with 1.25 s.g., the greatest changes were observed within the first hour of soaking. After that, even after 4 h of soaking, substantial amounts of H_2SO_4 remained unreacted. This means that after 1 h of soaking the rate of sulfation of the paste is slowed down substantially as a result of difficulties created by the newly formed sulfated structures.

3.2. Zonal processes during plate soaking forming different sub-layers across the plate thickness

Fig. 2 presents a micrograph of the cross-section of a plate after 4 h of soaking in 1.06 s.g. H_2SO_4 solution.

Three sub-layers (zones) of different colour can be distinguished:

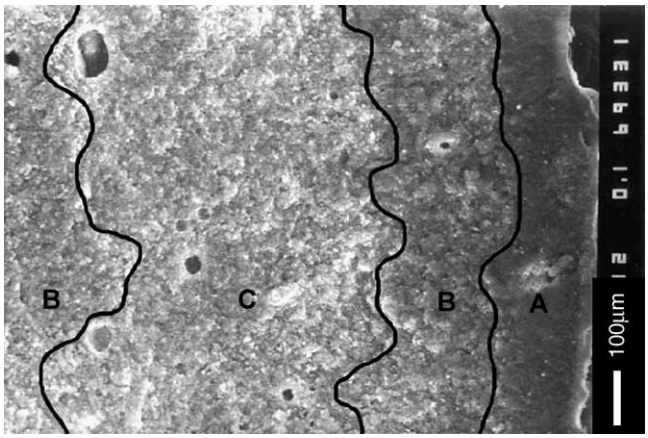

Fig. 2. A cross-section view of the plate after 4 h of soaking in 1.06 s.g. H_2SO_4 solution: (A) outer sub-layer; (B) intermediate sub-layer; (C) central (inner) sub-layer.

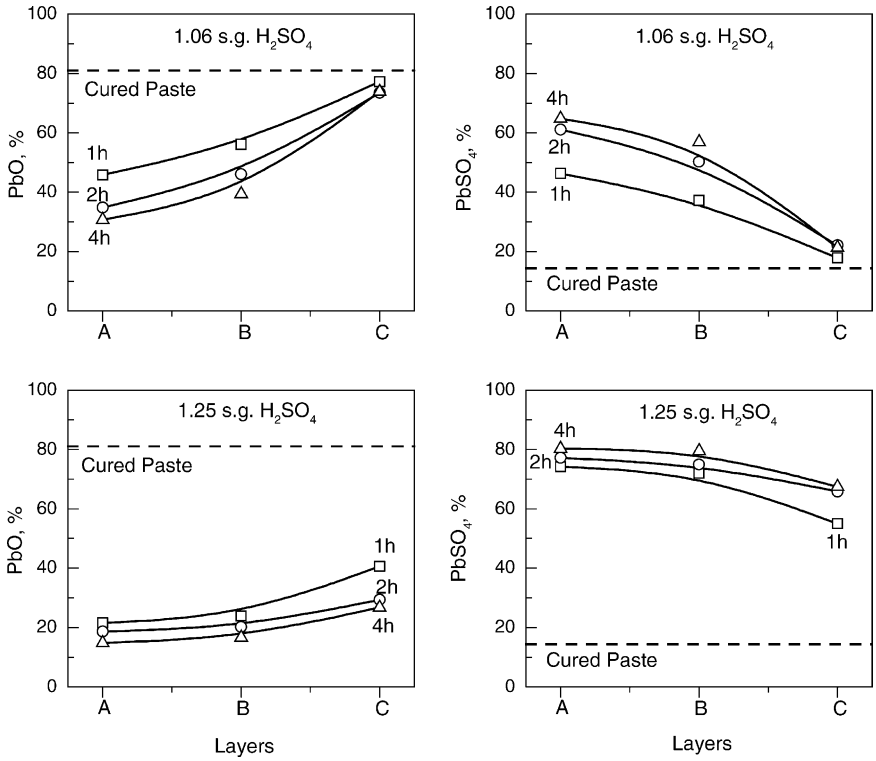

Fig. 3. Content of PbO and $PbSO_4$ in the three sub-layers (A–C) across the plate thickness after 1, 2 and 4 h of soaking in 1.06 and 1.25 s.g. H_2SO_4 solution.

A. *outer sub-layer*: contacting the bulk solution, dark grey in colour, with compact structure;
B. *intermediate sub-layer*: grey with white spots;
C. *central* (*inner*) *sub-layer*: light grey in colour with yellowish tint and white spots.

3.3. Chemical composition of the three sub-layers across the thickness of the plates soaked in 1.06 and 1.25 s.g. H_2SO_4 solution

Fig. 3 summarizes the results of the chemical analysis of samples from the three sub-layers. "*Cured paste*" stands for the content of $PbSO_4$ in 3BS as well as for PbO in 3BS and free PbO in the cured paste.

- The highest degree of sulfation is established in the outer sub-layer (A).
- At both H_2SO_4 concentrations, sulfation of the paste is most intense within the first hour of soaking.

Fig. 4 shows the average amount of $PbSO_4$ formed in the paste after 1, 2 and 4 h of soaking. The average amount is obtained from the sum of the $PbSO_4$ quantities formed in the three sub-layers across the plate thickness divided in three.

The degree of sulfation of the pastes soaked in 1.06 s.g. H_2SO_4 solution for 4 h reaches up to 47%, whereas the pastes soaked in 1.25 s.g. H_2SO_4 undergo 75% sulfation for the same time of soaking.

3.4. Changes in H_2O content in the paste particles during plate soaking in H_2SO_4 solution

According to the 3BS formula generally accepted in the literature the basic sulfate contains one water molecule: $3PbO{\cdot}PbSO_4{\cdot}H_2O$. In order to disclose the chemical processes that proceed between H_2SO_4 and 3BS, we have to establish whether or not some processes of paste hydration take place on plate soaking. During soaking the pH of the solution filling the paste pores in the central plate zone *C* is high as the H_2SO_4 is consumed in the outer and intermediate sub-layers, and hence 3BS and PbO may undergo hydration.

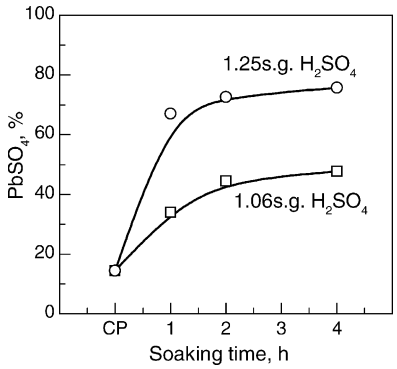

Fig. 4. Average $PbSO_4$ content formed in the plate during soaking in 1.25 and 1.06 s.g. H_2SO_4 solution.

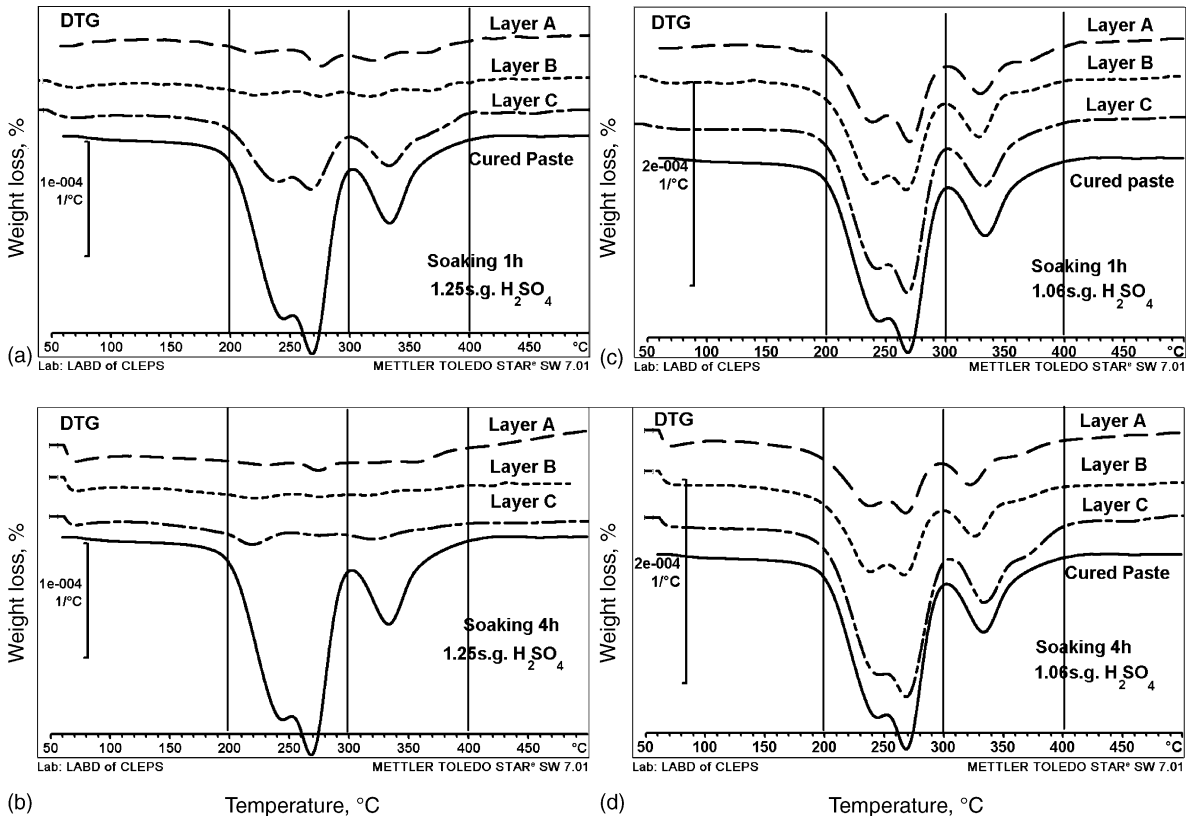

Fig. 5. Differential thermogravimmetric (DTG) curves of the weight losses with temperature increase for the outer (A), intermediate (B) and central (C) sub-layers after 1 and 4 h of soaking in 1.06 and 1.25 s.g. H_2SO_4 solution.

On heating the samples during the differential thermal gravimetric (DTG) measurements this hydrating water evaporates and the sample loses weight

Fig. 5 presents the obtained DTG curves giving the differential weight losses on temperature increase for the outer, intermediate and central sub-layers of samples taken after 1 and 4 h of soaking in H_2SO_4 with 1.06 and 1.25 s.g., respectively.

The following conclusions can be drawn from this figure:

- The DTG curve for the 3BS paste immediately after curing features a great low-temperature (200–300 °C) and a small high-temperature (300–400 °C) characteristic peaks. Within the former temperature interval we can distinguish clearly two peaks: at 240 and at 270 °C. These peaks are indicative of different types of water bonding in the 3BS particles of the paste.
- The characteristic peaks for 3BS disappear from the DTG curves for the *A* and *B* sub-layers within the first hour of soaking, and for the *C* sub-layer after 4 h of soaking in 1.25 s.g. H_2SO_4 (Fig. 5a and b). The 3BS crystals disintegrate under acid attack. After 1 h of soaking, the *C* sub-layer still contains some 3BS particles.

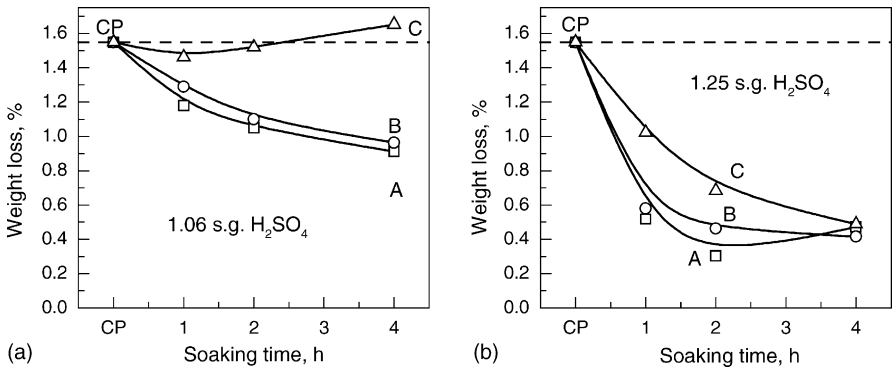

Fig. 6. Weight losses for the three sub-layers of the plate (A–C), determined through TGA measurements after different times of soaking in 1.06 and 1.25 s.g. H_2SO_4 solution.

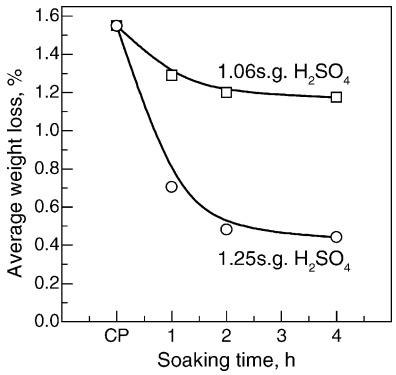

Fig. 7. Average weight losses for the samples, determined through TGA measurements, as a function of time of soaking in 1.06 and 1.25 s.g. H_2SO_4 solution.

- It is evident from Fig. 5c and d that during soaking in 1.06 s.g. H_2SO_4 solution, the characteristic peaks for 3BS are preserved, though less intensive, even after 4 h of soaking. 3BS crystals remain not much affected by sulfation.

Fig. 6 shows the weight losses (as measured by thermal gravimmetry (TG)) for the three sub-layers on heating the samples after different times of soaking. When the plates are soaked in 1.06 s.g. H_2SO_4 solution (Fig. 6a), the weight losses of sub-layers *A* and *B* decrease slightly. The weight loss of the central sub-layer *C* after 4 h of soaking is greater even than that of the cured paste. This indicates that some hydration processes take place in the central sub-layer of the plates during soaking. Probably, the PbO and $3PbO{\cdot}PbSO_4{\cdot}H_2O$ phases undergo hydration.

Fig. 6b presents the weight losses for the three sub-layers on heating the samples soaked in 1.25 s.g. H_2SO_4 solution. After 4 h of soaking the weight losses for the three sub-layers are almost the same (0.4%). Despite the still high H_2SO_4 concentration (1.105 s.g., Fig. 1), no sulfation of PbO proceeds or, if any, it proceeds at a very low rate. Fig. 5 evidences that the characteristic endothermic peaks for 3BS disappear from the curves for the *A* and *B* sub-layers after 1 h of soaking in 1.25 s.g. H_2SO_4, i.e. in these layers the 3BS phase has decomposed. The same effect is also observed in the *C* sub-layer after 4 h of soaking. On the other hand, Fig. 6 indicates that all three sub-layers contain H_2O, though in very small amounts. Hence, the oxides and basic lead sulfates in the soaked pastes have undergone hydration and have been isolated from direct contact with the H_2SO_4 solution.

Fig. 7 presents the average weight losses of the samples as a function of time of soaking. On comparing the curves in Figs. 7 and 4 it can be seen that they are opposite in profile. The more sulfated the paste (Fig. 4), the smaller the water loss (Fig. 7), i.e. the lower the hydration of the oxides in the paste.

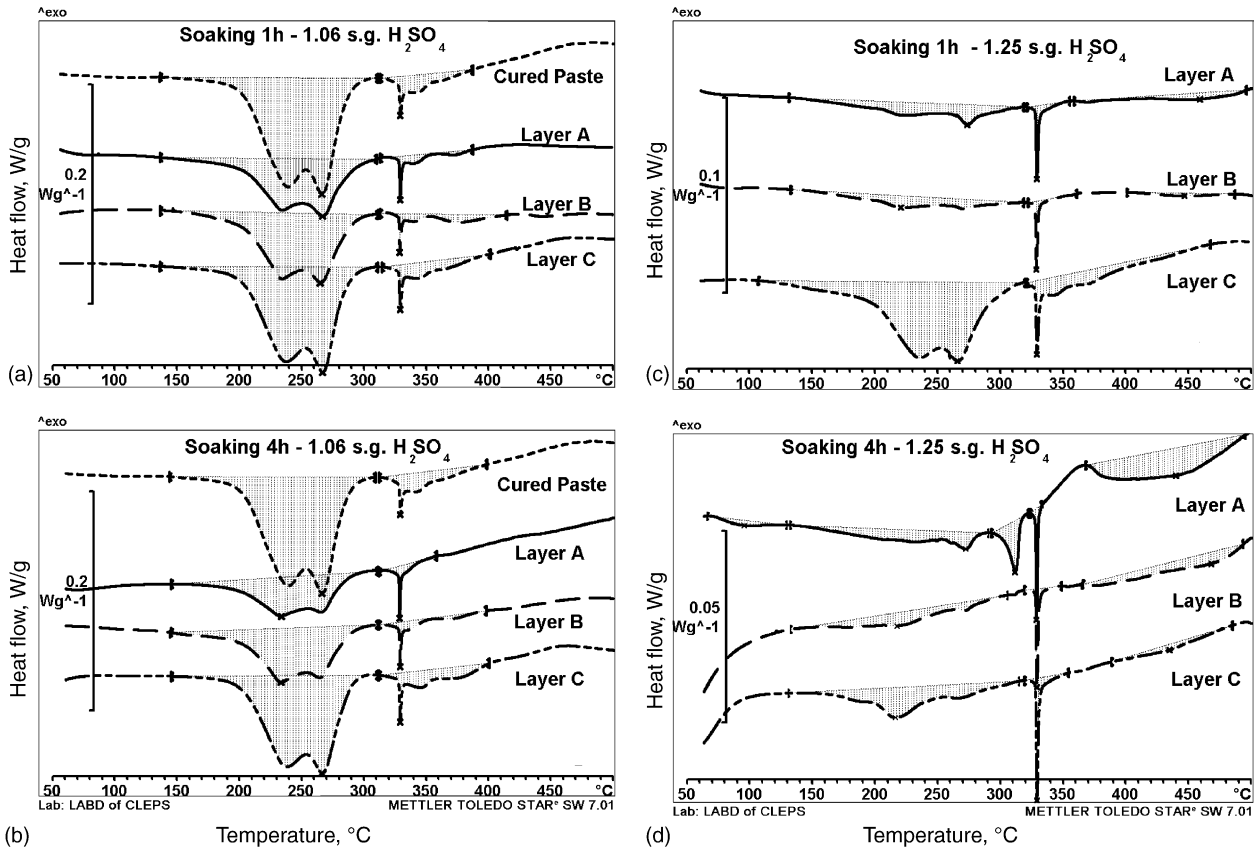

Fig. 8. DSC curves for samples taken from the three sub-layers across the plate thickness after 1 and 4 h of soaking in 1.06 and 1.25 s.g. H_2SO_4 solution.

3.5. Investigation of the dehydration phenomena in the pastes by differential scanning calorimetry (DSC)

On heating the samples at linearly increasing temperature the amount of evaporating water from the samples was measured through determining the energy of dehydration. Fig. 8 presents the DSC curves for samples taken from the three sub-layers of the plate after 1 and 4 h of soaking in 1.06 s.g. H_2SO_4 solution (Fig. 8a and b) or in 1.25 s.g. H_2SO_4 solution (Fig. 8c and d).

The basic endothermic peak of 3BS dehydration occurs between 170 and 300 °C and features two characteristic peaks at 240 and 270 °C, respectively (Fig. 8a–c, sub-layer *C*). A sharp peak appears at 330 °C, which reflects the energy for melting the lead that has remained unoxidized during the curing process. In the temperature region between 300 and 400 °C, two small endothermic peaks are observed with dehydration energy lower than 1.5 J/g (Fig. 8a and b). Except for the Pb peak, the DSC curves (Fig. 8) are similar to the DTG curves (Fig. 5), which means that they both reflect the same phenomena – the evaporation of water form the hydrated oxides and basic lead sulfates.

Fig. 8c and d shows that after the characteristic peaks for 3BS have disappeared from the DSC curves for the three sub-layers, some wide but shallow endothermic peaks appear instead. They are due to the evaporation of the hydrating water from the oxides and the hydrated $PbO{\cdot}PbSO_4$ (1BS) formed in the paste as an intermediate product of the sulfation of 3BS (see next paragraph).

The dehydration energies for the three sub-layers of the paste were summed up and divided by three in order to obtain the average energy of dehydration. The obtained values are presented in Fig. 9. The energy curves in Fig. 9 look very much the same as the curves in Fig. 7 reflecting the weight losses as determined through TGA analysis.

Fig. 10 presents the dehydration energy as determined from the DSC curves versus the water loss on heating as determined from the TGA curves. The dehydration energy for chemically prepared 3BS is also given in the figure. The obtained dependence yields a straight line passing through the beginning of the coordinate system. From the slope of this line

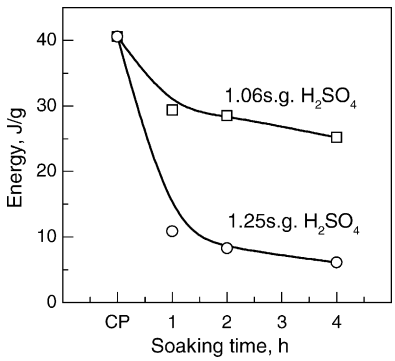

Fig. 9. Average dehydration energy for the samples of soaked pastes as a function of time of soaking in 1.06 and 1.25 s.g. H_2SO_4 solution.

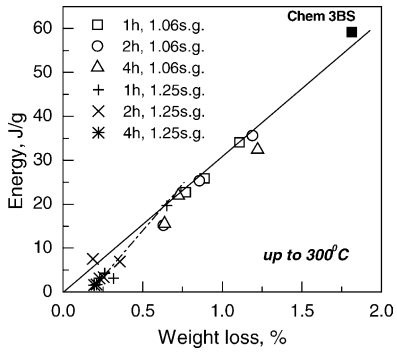

Fig. 10. Average dehydration energy (DSC measurement) versus average weight loss (TGA measurement) on heating samples of pastes soaked in 1.06 and 1.25 s.g. H_2SO_4 solution.

we have determined that the dehydration energy for the 3BS paste is equal to 3.2 kJ/g (H_2O) in the paste. Fig. 10 shows also that at high degrees of paste sulfation, when soaked in 1.25 s.g. H_2SO_4 solution, the values for the dehydration energy lie below the straight line. The slope of the new line drawn through these points is steeper. This indicates that a greater amount of energy should be introduced for dehydration of the highly sulfated paste after the disintegration of the 3BS crystals. This may mean that the hydrated oxides are capsulated in $PbSO_4$ and hence more energy is required for the dehydration of these hydroxides.

In an attempt to determine whether the cured pastes contain carbonates and what is their influence on the DSC curves, a plate with cured 3BS paste was left in the air for 1 month and then set to DSC analysis. Another plate was left in a humid CO_2 atmosphere for 3 h and then analyzed through differential scanning calorimetry. And finally, the DSC profile of the hydrocerussite was plotted. The obtained DSC curves are presented in Fig. 11.

The DSC curve for hydrocerussite features a basic peak of decarbonation between 300 and 420 °C, and two smaller peaks between 230 and 300 °C. As the DSC curve for the

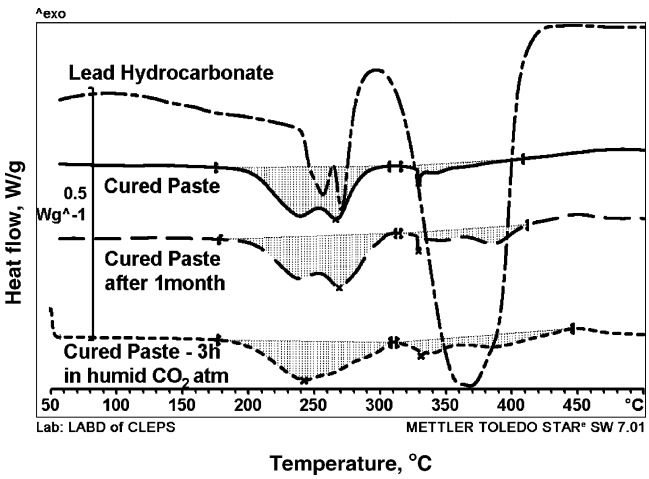

Fig. 11. DSC curves for: cured paste, cured paste after 1 month stay in air, cured paste after 3 h stay in humid CO_2 atmosphere, hydrocerrusite.

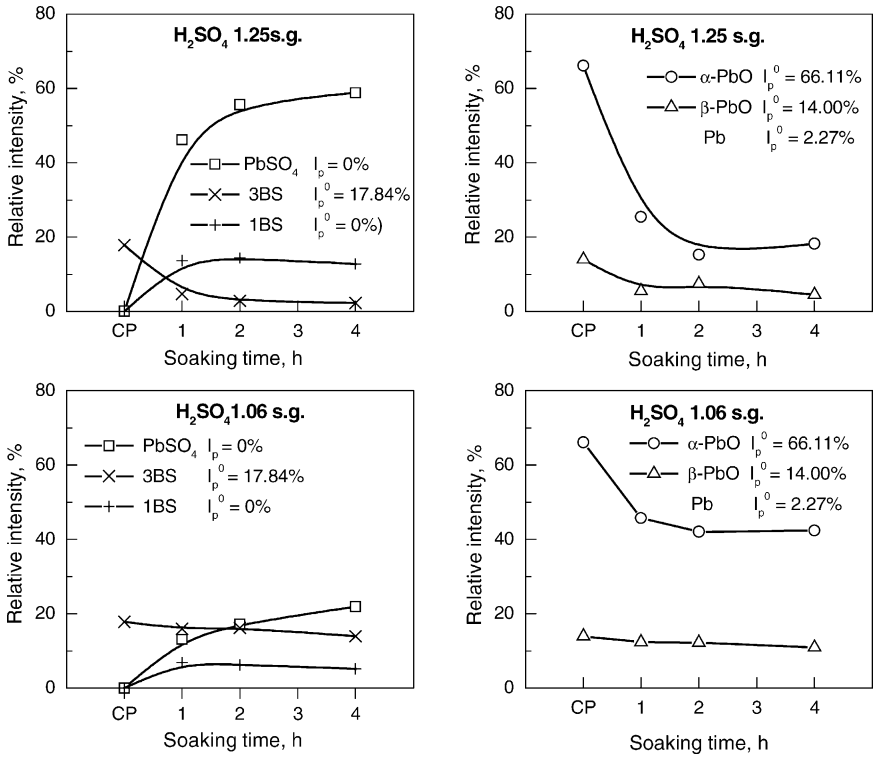

Fig. 12. Average phase composition of the paste after soaking in 1.25 or 1.06 s.g. H_2SO_4 solution for 1, 2 or 4 h. CP is the phase composition of the initial cured paste.

cured paste features two very small peaks (below 2 J/g) in the temperature range between 300 and 420 °C, and there is no process leading to energy consumption between 360 and 380 °C (where the maximum of the basic endothermic peak for hydrocerussite occurs), it can be concluded that the cured pastes used in our experiment are not carbonated. This is not the case, however, after prolonged stay of the plates in the air and in CO_2 atmosphere. Then a process of carbonation proceeds which is reflected in the increased upper temperature limit of the characteristic endothermic peak for 3BS as well as by the merger of the peaks at 240 and 270 °C into a single peak for the paste that had stayed in CO_2 atmosphere.

3.6. Changes in phase composition of the pastes during plate soaking

The changes in phase composition of the cured pastes during soaking in 1.06 or 1.25 s.g. H_2SO_4 solution for 1, 2 or 4 h were followed through X-ray diffraction analysis. The phase composition of the pastes was determined from the relative intensities of the characteristic diffraction lines for α-PbO (d = 0.281 nm), β-PbO (d = 0.308 nm), 3BS (d = 0.326 nm), $PbO{\cdot}PbSO_4$ (1BS) (d = 0.296 nm), $PbSO_4$ (d = 0.380 nm) and Pb (d = 0.285 nm). The relative intensity is the intensity of the characteristic diffraction line for a given phase versus the sum of the intensities of the characteristic lines for all phases in the sample. The phase composition of the cured paste comprises the following crystal phases: α-PbO: 66.1%, 3BS: 17.0%, β-PbO: 14.0% and Pb: 2.3%. The paste with the above composition was subjected to H_2SO_4 attack.

Fig. 12 presents the phase composition of the paste after 1, 2 and 4 h of soaking in 1.06 or 1.25 s.g. H_2SO_4 solution. During plate soaking H_2SO_4 reacts with α-PbO and β-PbO, and with 3BS forming mainly $PbSO_4$ and 1BS. When the H_2SO_4 concentration is 1.25 s.g., $PbSO_4$ is the predominant phase with about 15% of 1BS as well. When the plates are soaked in 1.06 s.g. H_2SO_4 solution, the quantities of $PbSO_4$ formed are commensurable with those of 3BS and the amount of the 1BS phase is about 8%. As the above substances are formed in three different pH regions, it follows that the pH of the pore solution in the different parts across the plate cross-section is different.

3.7. Changes in BET surface and porosity of the 3BS paste during soaking in 1.25 s.g. H_2SO_4 solution

The results of these investigations are presented in Fig. 13. After 4 h of soaking the BET surface area decreases by 35%, and the total pore volume by almost 60%, the mean pore radius being reduced from 0.20 to 0.07 μm. As the molar volume of $PbSO_4$ is greater than that of the components of the cured paste, and especially of PbO, sulfation will reduce the total pore volume of the paste.

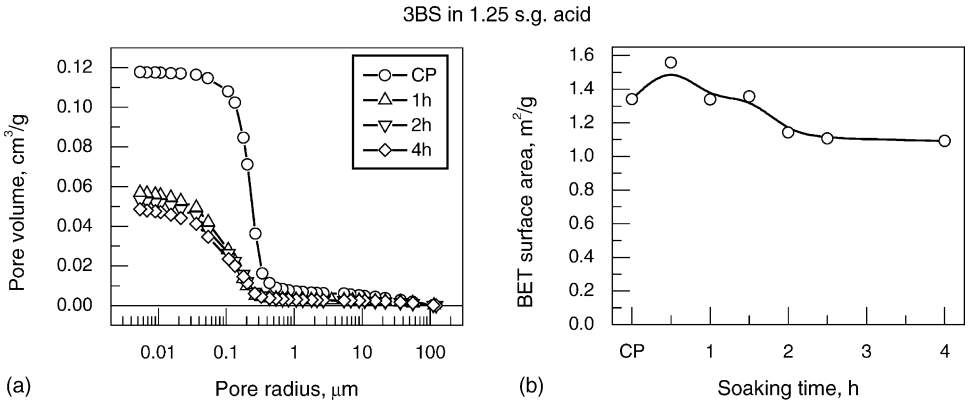

Fig. 13. (a) Pore volume distribution by pore radius for the cured pastes and after soaking in 1.25 s.g. H_2SO_4 solution for 1, 2 or 4 h. (b) Changes in BET surface of pastes immediately after curing (CP), and after soaking in 1.25 s.g. H_2SO_4 solution for different periods of time.

3.8. Structure of the paste after soaking

3.8.1. Structure of the outer zone of the plate after soaking

Fig. 14 shows the paste structure and the crystal morphology in the outer plate zones after 2 h of soaking in 1.25 s.g. H_2SO_4 solution. The picture in Fig. 14b features the structure of the plate surface. The outer sub-layer is more compact (Fig. 14a) and consists of $PbSO_4$ crystals and remnants of unreacted paste particles (Fig. 14b). The large $PbSO_4$ crystals have formed as a result of recrystallization processes: dissolution of the small crystals and growth of large ones. The process of $PbSO_4$ recrystallization was discussed in Ref. [15]. Obviously, the processes of sulfation and of $PbSO_4$ recrystallization change substantially the pore system of the soaked paste, which is also evident from Fig. 13a.

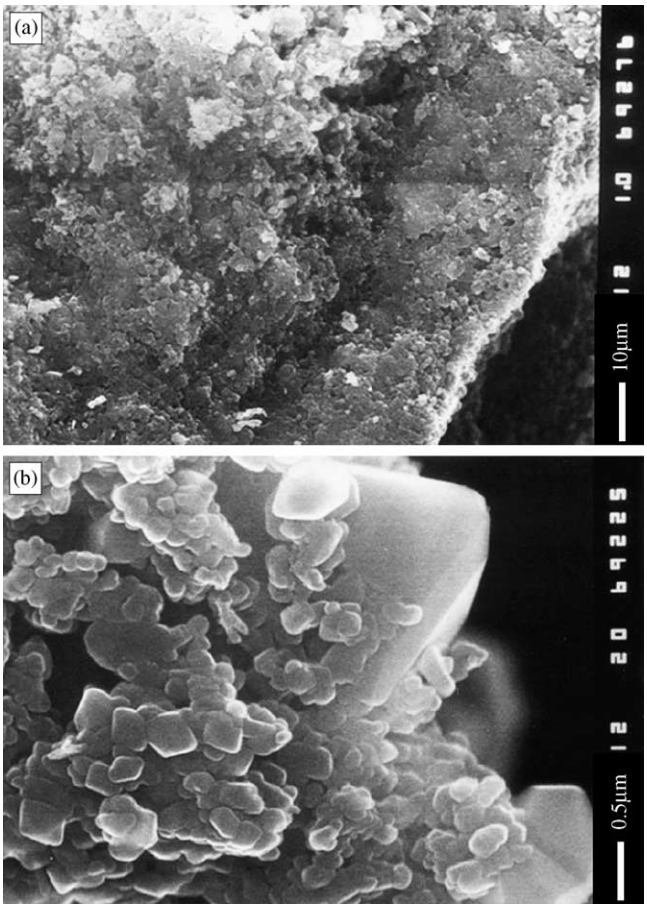

Fig. 14. SEM micrograph of the structure and crystal morphology of the outer sub-layer of a plate soaked in 1.25 s.g. H_2SO_4 solution for 2 h: (a) structure of the outer plate sub-layer; (b) crystals on the plate surface contacting the bulk solution.

3.8.2. Structure of the central zone of the plate after soaking

SEM pictures of the central zone *C* after soaking in 1.25 s.g. H_2SO_4 solution for 1 h are presented in Fig. 15. Most of the paste particles have remained unaffected by sulfation, but a process of rounding off and merging of the 3BS and PbO particles has started, which is probably due to hydration of the crystal surface (Fig. 15b). Besides, some needle-like particles are observed with crystal shape characteristic for 1BS (Fig. 15a and b).

3.8.3. Structure of the intermediate plate zone

Fig. 16 shows pictures of the paste in the intermediate plate zone, where there are pores with large radii. $PbSO_4$ crystals with well pronounced walls, edges and apexes (Fig. 16a) or long needle-like crystals of 1BS (Fig. 16c, upper right part) are formed on the pore walls. The $PbSO_4$ crystals may form a layer over the pore walls. The distance between the $PbSO_4$ crystals in this layer may reach membrane sizes and thus the process of sulfation may stop because of impeded H_2SO_4 transport through the membrane pores. Most probably, this process is responsible for the slowed sulfation of the paste on soaking. Water passes through the membrane pores only and the formation of hydrates of the lead oxides and of the basic lead sulfates occurs in those regions of the cured paste that are isolated from the H_2SO_4 solution by the $PbSO_4$ membrane formed on the surface of the large pores.

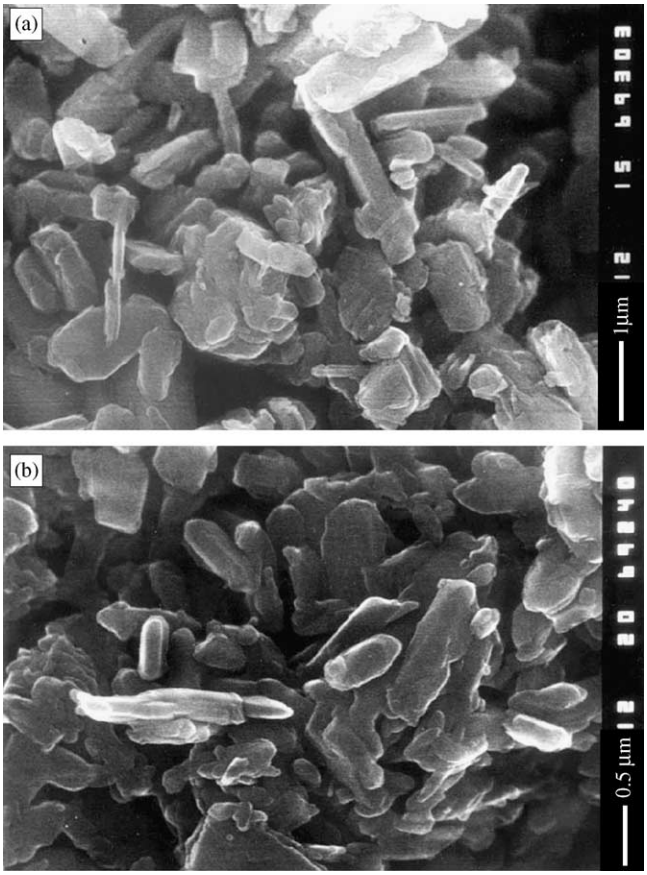

Fig. 15. Structure of the central plate zone after 1 of soaking in 1.25 s.g. H_2SO_4 solution. The layer is but very slightly affected by sulfation.

3.8.4. *Structure of the paste/grid interface obtained after soaking of positive plates in H_2SO_4 solution*

Fig. 17 presents pictures of the interface structure. The grid was stretched to allow a better view of the sub-layers across its thickness.

The paste/grid interface consists of the metal surface with the corrosion layer (CL) formed as a result of oxidation of the grid during plate curing and the paste layer adjacent to the corrosion layer. The CL comprises PbO at its interface with the metal surface and a partly hydrated lead oxide sub-layer at its interface with the paste [14].

Fig. 18 shows SEM pictures of the corrosion layer, which has reacted with H_2SO_4. The grid was stretched and the cross-section of the corrosion layer and its connection with the metal grains can be seen in Fig. 18a and c. Fig. 18b features individual $PbSO_4$ particles, formed as a result of recrystallization processes, and small $PbSO_4$ nuclei.

Fig. 18c and d shows a profile and en face views of the $PbSO_4$ layer comprising large elongated shapeless particles which have formed along the path of the H_2SO_4 flow on the surface of the CL. The formation of this particular type of $PbSO_4$ particles was found to occur when the concentration of H_2SO_4 versus Pb^{2+} is very high (or vice versa) [15].

Fig. 19 illustrates the case when the thickness of the CL is small. The H_2SO_4 flow reacts with this thin CL over the

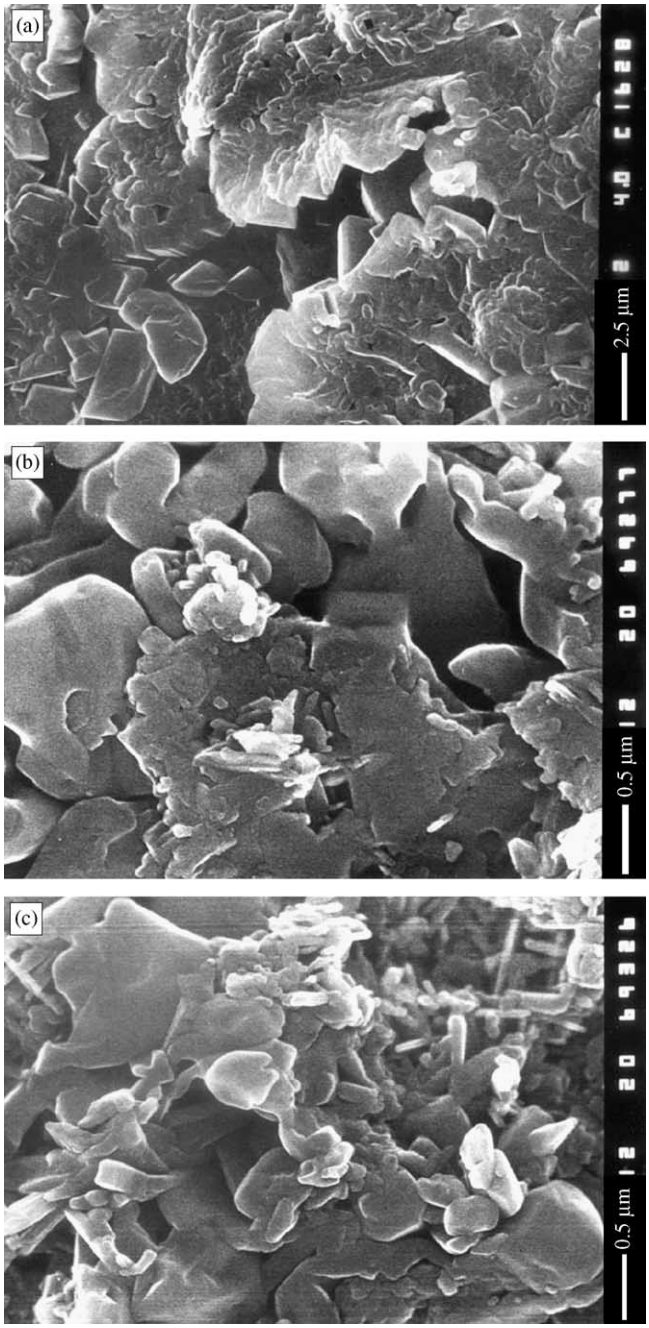

Fig. 16. SEM micrograph of the intermediate plate sub-layer containing large pores. $PbSO_4$ crystals form a layer on the walls of the large pores.

metal grains and the inter-grain layers. The inter-grain layer is composed of $(Pb_{(1-x)}Sn_x)_3Ca$ and is obtained as a result of segregation of Sn and Ca from the bulk of the metal grains to their boundaries [13,16]. The increased concentration of Ca in this layer facilitates the formation of $CaSO_4$ nuclei onto which $PbSO_4$ is deposited and grows into regular crystal shapes (Fig. 19a). When, however, Sn alone has segregated in the inter-grain layer, it dissolves during soaking and caverns are formed in the inter-grain space between the paste and the metal surface (Fig. 19b). These caverns impair the

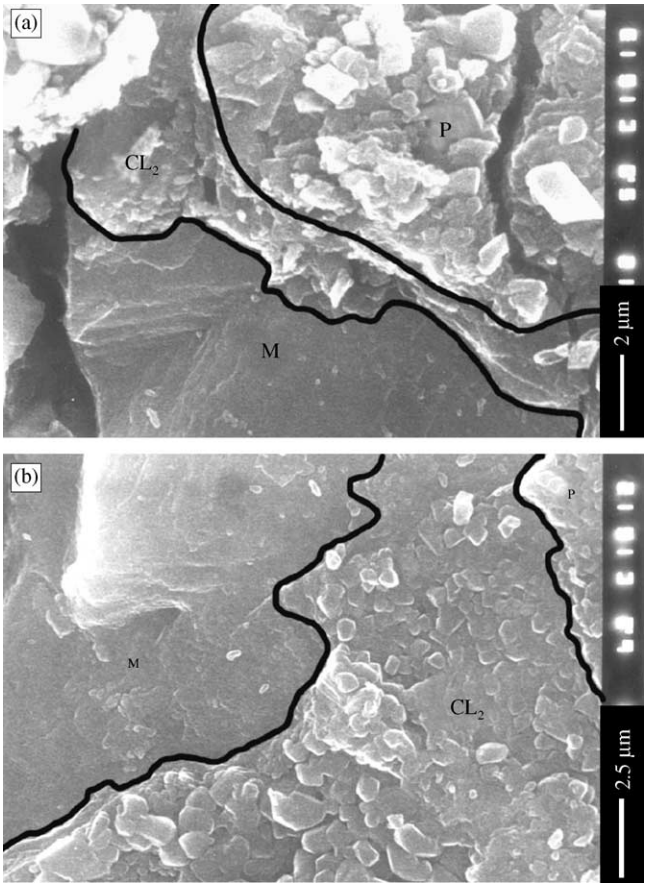

Fig. 17. Structure of the grid/paste interface: M stands for the metal surface; CL for corrosion layer; P for the paste that is partially sulfated.

contact paste/grid. Hence, the process of plate curing should be conducted under such conditions that allow the formation of a thick corrosion layer, which would prevent it from being fully sulfated and thus the access of H_2SO_4 to the metal will be impeded. As the rate of corrosion of PbSnCa grids is very low, the conditions of curing of such plates play a key role for the life of the batteries.

Fig. 20 presents micrographs of an interface zone reached by a highly diluted H_2SO_4 flow. Only at some sites, small $PbSO_4$ crystals have formed (Fig. 20a). Fig. 20b shows a picture of the paste layer contacting CL with pores of different sizes. In the zones with small pore radii the products of hydration and sulfation fill up these small pores. When the pores are plugged by the products of soaking ($PbSO_4$ membrane), the interface looks like a continuous (uninterrupted) layer (Fig. 20b).

3.9. Mechanism of the reactions that proceed during soaking of 3BS pastes

Liptay and Sors [14] mixed increasing amounts of H_2SO_4 with one and the same amount of leady oxide. They determined continuously the phase composition of the obtained pastes until a stoichiometric ratio $H_2SO_4/PbO = 1$ was reached. This ratio corresponds to the full consumption of the initial reagents for the reaction expressed by the following stoichiometric equation:

$$PbO + H_2SO_4 = PbSO_4 + H_2O \quad (1)$$

The phase composition of the paste was determined immediately after its preparation and 24 h later. Based on the data presented in Ref. [14] we plotted the dependence of phase composition of the paste as a function of the increasing H_2SO_4/PbO ratio from 3 to 100% (Fig. 21).

Fig. 21 indicates that on increasing the amount of H_2SO_4 versus that of PbO, the successive reactions represented by the following general chemical equations proceed:

$$4PbO + H_2SO_4 \rightarrow 3PbO \cdot PbSO_4 \cdot H_2O \quad (2)$$

$$3PbO \cdot PbSO_4 \cdot H_2O + H_2SO_4 \rightarrow 2(PbO \cdot PbSO4) + H_2O \quad (3)$$

$$PbO \cdot PbSO_4 + H_2SO_4 \rightarrow 2PbSO_4 + H_2O \quad (4)$$

The maximum amount of 3BS is formed at H_2SO_4/PbO = 33%, whereas at H_2SO_4/PbO = 75% mostly 1BS is formed. Even at H_2SO_4/PbO = 100%, the paste does not transform completely to $PbSO_4$. Such is the picture of the processes that take place during paste preparation.

The cured paste is a porous mass composed of PbO and 3BS, and when soaked, H_2SO_4 gets into the pores of this mass. The reactions of sulfation proceed between the surface of the PbO and 3BS particles, and the H_2SO_4 in the paste pores. These processes are similar to the ones presented in Fig. 21. The H_2SO_4/PbO ratio decreases in the depth of the plate, because part of the H_2SO_4 reacts and water is formed as a result of the sulfation of the PbO, 3BS and 1BS phases. The SEM pictures evidence that the processes of sulfation of the paste and of the paste/grid interface proceed at different rates in the different parts of the plate volume, and lead to the formation of different phases in the different micro-regions of the paste.

The DSC, TGA and DTG curves in Figs. 5, 6 and 8 show that some hydration processes proceed during sulfation of the paste. Probably, PbO, 3BS and 1BS are hydrated first, and the obtained hydrated products undergo sulfation, for example through the following reactions:

$$3PbO \cdot PbSO_4 \cdot H_2O + 3H_2O \rightarrow 3Pb(OH)_2 \cdot PbSO_4 \cdot H_2O \quad (5)$$

$$3Pb(OH)_2 \cdot PbSO_4 \cdot H2O + H_2SO_4 \rightarrow 2Pb(OH)_2 \cdot PbSO_4) + 3H_2O \quad (6)$$

Part of the $Pb(OH)_2 \cdot PbSO_4$ is dehydrated

$$Pb(OH)_2 \cdot PbSO_4 \rightarrow PbO \cdot PbSO_4 + H_2O \quad (7)$$

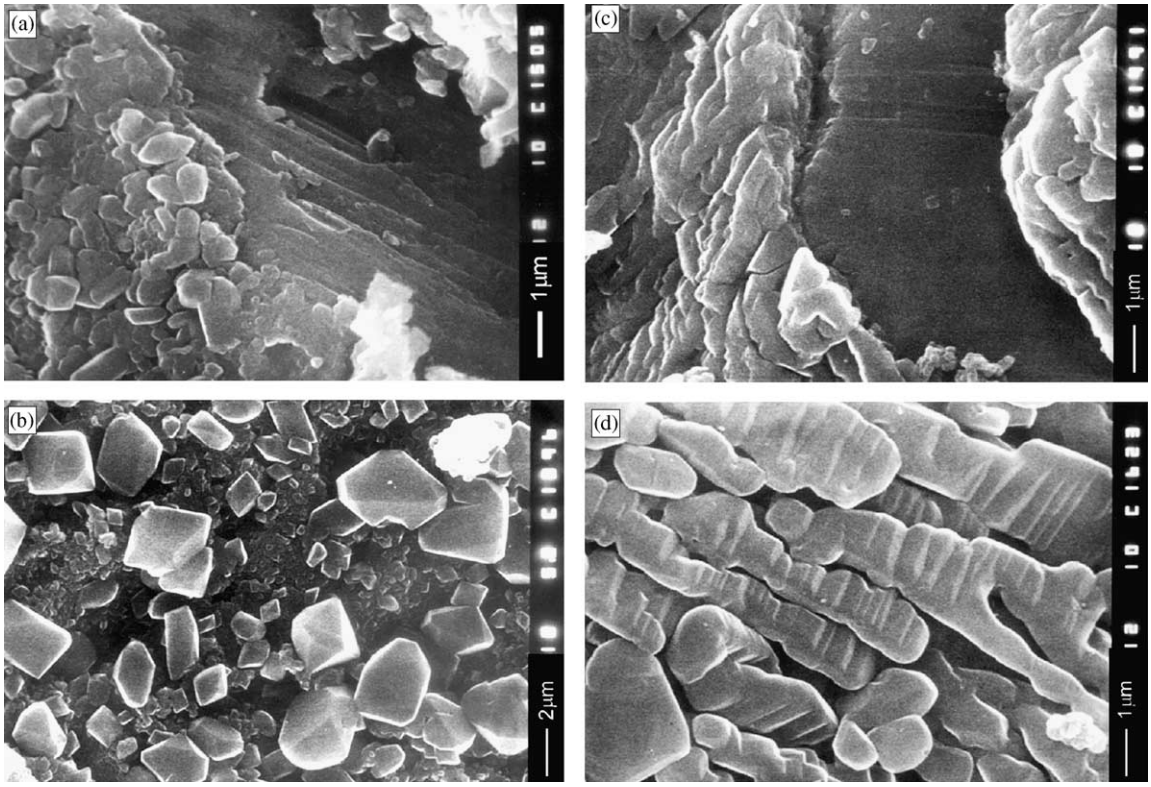

Fig. 18. SEM micrographs of the corrosion layer that has undergone sulfation. The grid has been stretched to tear off the corrosion layer.

the 1BS phase being registered by X-ray diffraction, and another part is sulfated further:

$$Pb(OH)_2 \cdot PbSO_4 + H_2SO_4 \rightarrow 2PbSO_4 + H_2O \quad (8)$$

The great amount of $PbSO_4$ in the *A* and *B* sub-layers even after soaking in 1.06 s.g. H_2SO_4 solution, indicates that the reaction of sulfation of $Pb(OH)_2 \cdot PbSO_4$ proceeds faster than the reaction of dehydration.

The ratio between the rates of the reactions of hydration and sulfation of the lead oxide and of the basic sulfates will depend on the radii of the paste pores. If the mean pore radius is smaller than a certain critical value, the diffusion flow of H_2SO_4 in the pores is very small and the reactions of hydration will proceed at a higher rate than those of sulfation. Hence, micro-volumes of hydrated oxides and basic lead sulfates will be formed (Fig. 20b). On the contrary, when the pores have large radii, the diffusion flow of H_2SO_4 in the pores will be large and the rate of the reactions of sulfation of the various hydrates will be much higher than that of the hydration reactions, and mostly $PbSO_4$ will form in these micro-regions of the paste and of the paste/grid interface (Figs. 14, 16 and 18).

On comparing the phase compositions of the paste immediately after curing and after 24 h of soaking (presented in Fig. 21), it becomes evident that some recrystallization processes take place in the paste, as a result of which the content of crystal $PbSO_4$ increases from 8 to 42%. Such recrystallization processes proceed also during soaking of the plates.

3.10. Influence of the soaking processes on battery cycle life performance

Three capacity tests were performed at 20 h rate of discharge. All batteries exhibited over 100% of the rated capacity calculated at 50% utilization of the PbO_2 active mass. Fig. 22 presents the capacity versus cycle number dependencies for the batteries under test.

The concentration of the H_2SO_4 solution during soaking and formation exerts a stronger influence than the duration of soaking. The batteries soaked in 1.06 s.g. H_2SO_4 solution have longer cycle life than those soaked in 1.25 s.g. H_2SO_4. The time of soaking has a weaker effect on battery life as the basic processes are completed within the first hour of soaking. During this time the three zones across the plate thickness are formed.

3.11. Influence of grid alloy, soaking conditions and operation mode on battery cycle life

In a previous investigation of ours on soaking of 3BS pastes we established that the cells soaked and formed in 1.15 or 1.25 s.g. H_2SO_4 solutions have longer cycle life than the batteries soaked and formed in 1.05 s.g. H_2SO_4 solution [6]. In the present investigation, we have established that the

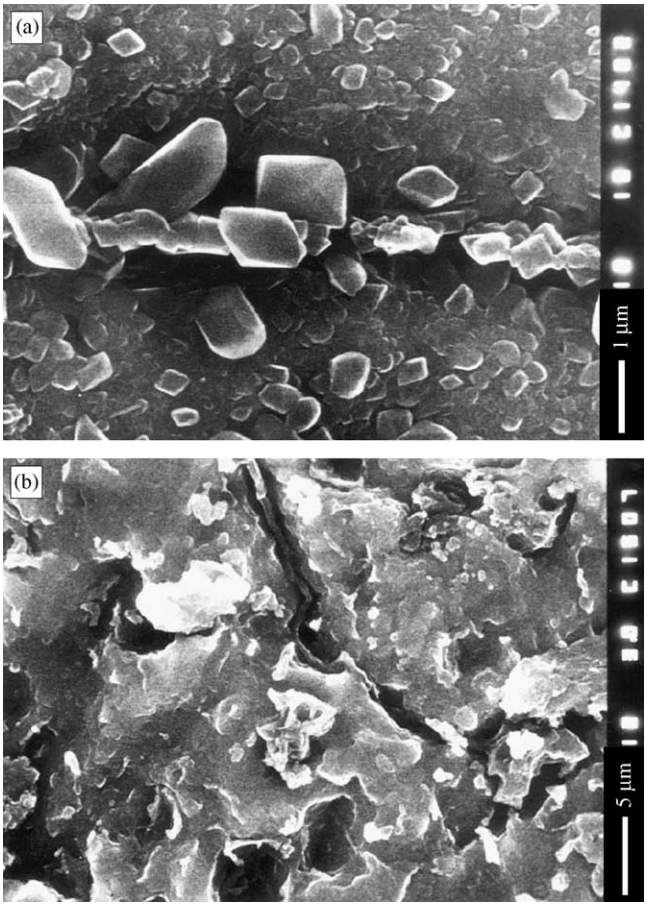

Fig. 19. Structure of the grid/paste interface when the corrosion layer is very thin: (a) H_2SO_4 reacts with the inter-metalgrain layer of $(Pb_{(1-x)}Sn_x)_3Ca$ forming $PbSO_4$ crystals; (b) caverns form between the corrosion layer and the paste at some sites.

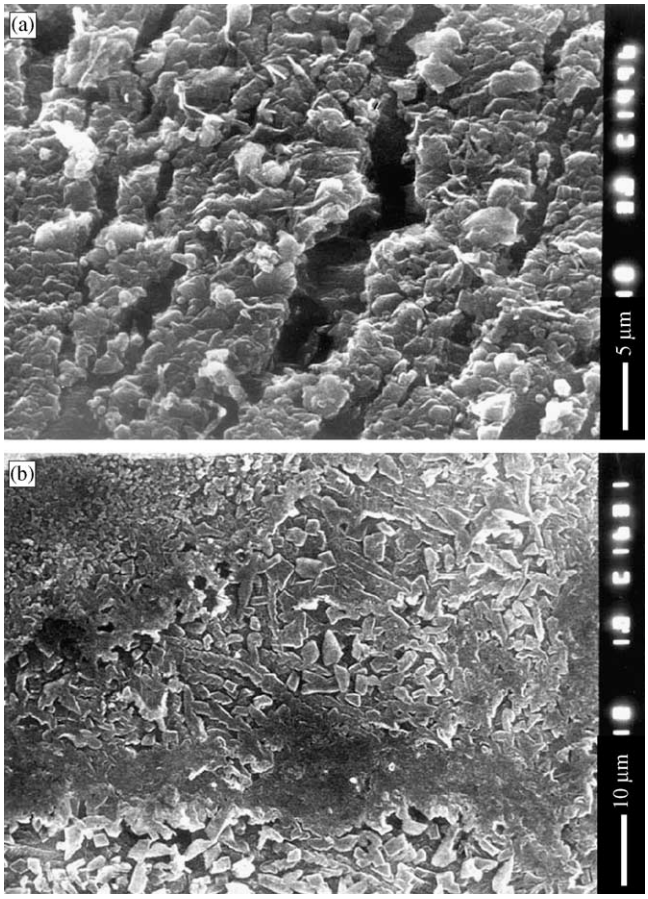

Fig. 20. Structure of the interface accessed by a highly diluted H_2SO_4 flow: (a) the grid has been stretched before the SEM observations to tear off the corrosion layer; (b) structure of the interface grid/pate of a soaked plate containing pores with radii of different sizes.

batteries soaked in 1.06 s.g. H_2SO_4 solution has longer cycle life than those soaked and formed in 1.25 s.g. H_2SO_4 solution.

What were the conditions of plate production and of battery tests in the above investigations and how did they influence the battery cycle life performance?

(a) In the study reported in Ref. [6] we used PbSbSnAs grids and in the present investigation the grids are of PbSnCaAl alloy. The different grid alloys used influence the structure and properties of the interface grid/corrosion layer/paste. The corrosion layer formed during curing on

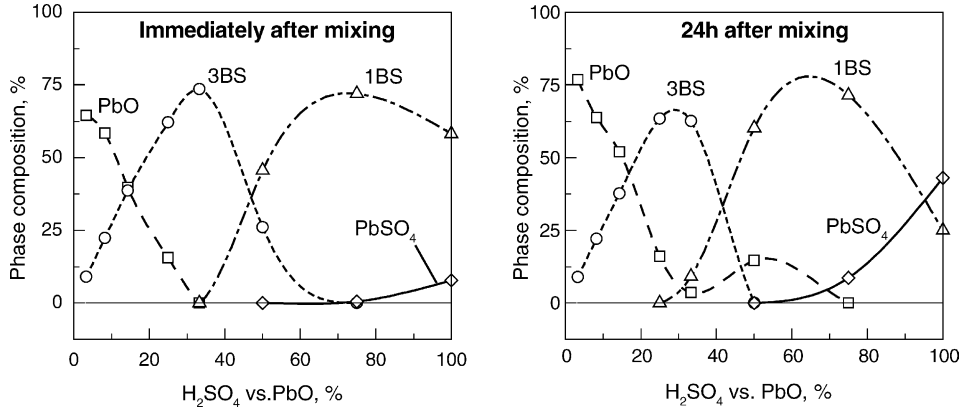

Fig. 21. Phase composition of pastes prepared with different amounts of H_2SO_4 vs. PbO. The values 100% on the abscissa corresponds to H_2SO_4:PbO = 1:1. The curves are plotted using data reported in Ref. [14].

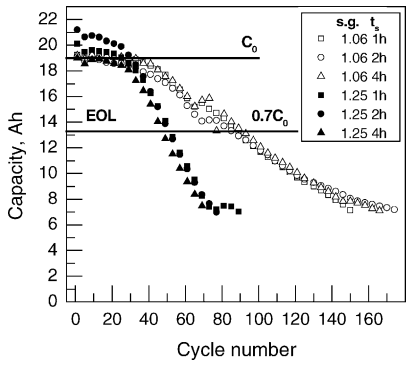

Fig. 22. Battery capacity vs. number of charge–discharge cycles for batteries soaked and formed in 1.06 or 1.25 s.g. H_2SO_4 solution.

the PbSnCa grids is thinner than that on the PbSbSn grids. The former CL is more easily sulfated during soaking. This affects the structure of the interface, which may limit the cycle life of the battery.

(b) In our earlier investigation [6] the percent share of sulfated paste after 1, 2 and 4 h of soaking was smaller than that of the sulfated paste in the present work. This was due to the different H_2SO_4/paste ratio. The phase composition of the paste during plate formation affects the structure of the lead dioxide active mass obtained. The PAM structure is one of the factors that determine the capacity of the battery and thus its cycle life, too.

(c) The tests of the batteries in our previous work [6] were conducted according to the SLI test protocol DIN43539/2, cycling was performed at 40 °C and the end-of-life was determined through a CCA test at −18 °C with current $I = 5\ C_{20}$ A. In the present investigation the batteries were cycled according to the traction battery test program at 25 °C, 3 h rate of discharge and 115% overcharge versus the preceding discharge cycle. The end-of-life criterion was when the batteries failed to deliver 75% of their rated capacity.

The above comparison of the results indicates that the H_2SO_4 concentration for plate soaking and battery formation should be selected taking into account the grid alloy and the type and application of the batteries in order to ensure optimum cycle life performance.

Acknowledgements

The present research was sponsored by the Advanced Lead Acid Battery Consortium (ALABC), a program of the International Lead Zinc Research Organization, Inc. (ILZRO). The authors want to extend their special thanks to both organizations as well as to Dr. P. Moseley for his support for the present work.

References

[1] D. Pavlov, J. Electroanal. Chem. 72 (1976) 319.
[2] D. Pavlov, G. Papazov, J. Electrochem. Soc. 127 (1980) 2104.
[3] G. Papazov, J. Power Sources 18 (1986) 337.
[4] V.H. Dodson, J. Electrochem. Soc. 108 (1961) 401.
[5] J. Burbank, J. Electrochem. Soc. 113 (1966) 10.
[6] D. Pavlov, S. Ruevski, T. Rogachev, J. Power Sources 46 (1993) 337.
[7] M.T. Lin, Y.Y. Wang, C.C. Wan, Elecrtochim. Acta 31 (1986) 565.
[8] I. Dreier, F. Saez, P. Scharf, R. Wagner, J. Power Sources 85 (2000) 117.
[9] L.T. Lam, A.M. Veechio-Sadus, H. Ozgun, D.A.J. Rand, J. Power Sources 38 (1992) 87.
[10] L.T. Lam, H. Ozgun, L.M.D. Craswick, D.A.J. Rand, J. Power Sources 42 (1993) 55.
[11] S. Grugeon-Dewaelle, J.B. Lariche, J.M. Taraskon, H. Delahayr-Vidal, L. Torcheux, J.P. Vaurjoux, F. Henn, A. de Guibert, J. Power Sources 64 (1997) 71.
[12] L. Torcheux, J.P. Vaurjoux, A. de Guibert, J. Power Sources 64 (1997) 81.
[13] D. Pavlov, M. Dimitrov, T. Rogachev, L. Bogdanova, J. Power Sources 113 (2003) 137.
[14] G. Liptay, L. Sors, Thermochim. Acta 14 (1976) 279.
[15] D. Pavlov, I. Pashmakova, J. Appl. Electrochem. 17 (1987) 1075.
[16] L. Bourden, J.P. Hilger, J. Hertz, J. Power Sources 33 (1991) 27.